Egyptian Geophysical Society
EGS Journal, Vol. 9, No. 1, 37-50 (2011)

GROUNDWATER RESOURCES AND POTENTIAL IN WADI GARAWI, EAST EL TEBEN, EASTERN DESERT, EGYPT: INFERENCES FROM GEOELECTRICAL INVESTIGATIONS

A.M.M. Al Temamy
Geophysics Department, Desert Research Center.

مصادر المياه الجوفية وإمكانياتها بوادى جراوى، شرق التبين،الصحراء الشرقية ، مصر: استدلال من الاستكشاف الجيوكهربى

الخلاصة: التنمية المستدامة لخزانات المياة الجوفية تتطلب مصدر دائم للتغذية كما أن ميكانكية التغذية ومصدرها بمنطقة الدراسة محل سؤال لذا فإنه فى هذه الدراسة تم استخدام الطرق الجيوكهربية للإجابة على هذا السؤال بوادى جراوى . لتحقيق الهدف من هذه الدراسة تم إجراء عشرين جسة جيوكهربية عمودية وقطاعين للجيوكهربية المقطعية ؛ من نتائج تحليل الجسات الجيوكهربية والقطاعات المشيدة تم التعرف على ثلاث وحدات جيوكهربية رئيسية (أ ، ب ، جـ) التى تكافىء رواسب عصر الرباعى والبلايوسين والايوسين على الترتيب ؛ تم التعرف على ثلاث طبقات حاملة للمياة الجوفية وهى (أ٣) ، وتمثل الرواسب الوديانية لعصر الرباعى الطبقة (ب ٢) وتمثل الحجر الرملى لعصر البلايوسين الطبقة (جـ١) وتمثل الحجر الجيرى لعصر الايوسين. نتائج تحليل قطاعى الجيوكهربية المقطعية متوافقة مع نتائج تحليل الجسات الجيوكهربية حيث يقل سمك خزان البلايوسين فى الجنوب بالمقارنة بالجزء الشمالى وكذلك التأثير التركيبى غرب منطقة الدراسة والمسئول عن وجود خزان البلايوسين فى الناحية المقابلة لطبقة الطين لنفس العصر . تساهم الفوالق التركيبية على تواجد المياه الجوفية بمنطقة الدراسة حيث تم التعرف على خمسة فوالق طبيعية لها دور فى تغذية الخزانات الجوفية فى بعض المناطق بمرور المياة من خلالها كما أنها تعمل كحدود غير مُنفذة فى مناطق أخرى ، وأيضاً لها تأثير واضح فى زيادة سمك خزان العصر الرباعى فى الجزء الغربى بالمقارنة بالجزء الشرقى ؛ وُجَد أن خزان العصر الرباعى فى الجزء الغربى يتغذى من نشع المياة لنهر النيل الذى له نفس منسوب مستوى النهر ، ومن الناحية الأخرى يتغذى هذا الخزان من مياة السيول والأمطار فى الجزء الشرقى. بينت الدراسة وجود اتصال هيدروجيولوجى بين الخزانات المختلفة نتيجة لتأثير الفوالق التركيبة مثل الذى بين خزان العصر الرباعى وخزان البلايوسين فى الغرب وكذلك بين خزان البلايوسين والحجر الجيرى الحامل للمياه والذى يتبع عصر الايوسين فى الشرق كما أن للتأثير التركيبى دوراً فى إزاحة طبقة الطين (ب٣) بوسط منطقة الدراسة وكذلك النسبة العالية للطين المتداخل مع الرمال فى شمال منطقة الدراسة تقسم مصادر التغذية إلى نطاقين : تغذية دائمة من خزان الرباعى الذى يتغذى من نشع نهر النيل فى الغرب ، وتغذية موسمية من صخور الحجر الجيرى من عصر الايوسين الذى يتغذى من خلال التراكيب والشقوق العميقة ، وللفوالق التركيبة دور فى اختزال سمك خزان البلايوسين المزاح لأعلى إلى قيم صغيرة (٨،٥م) وعلى ذلك إمكانات المياه الجوفية يتوقع أن تكون ضعيفة ؛ كما أن الخزان الرباعى لم يتم التعرف عليه فى الجسات الكهربية الجنوبية نتيجة للتأثير التركيبى . بما أن سمك خزان العصر الرباعى يزيد فى الجزء الغربى من منطقة الدراسة و تغذية هذا الخزان من نشع نهر النيل الذى يضمن مصدر للتغذية الدائمة للمياه الجوفية كما أن خزان البلايوسين فى الجزء الغربى من منطقة الدراسة يتغذى من خزان العصر الرباعى وعلى هذا الأساس فان الجزء الغربى يعتبر أفضل الأماكن للتنمية المستدامة بمنطقة الدراسة.

ABSTRACT: *Sustainable development of groundwater aquifers requires a permanent source of groundwater and a mechanism for recharging the aquifer. In this study, geoelectric methods were used to address the sources of groundwater and the mechanics of recharge in Wadi Garawi. To fulfill the objective of this study twenty Vertical Electrical Soundings and Two-Dimensional electrical imaging profiles were measured. Results of the VES data and the constructed cross-sections indicate the presence of three main geoelectrical units (A, B and C) which correspond to Quaternary, Pliocene and Eocene deposits, respectively. Three water-bearing formations in the area of study are detected. These formations are represented by geoelectrical layer "A3" (a part of the Quaternary alluvial deposits), geoelectrical layer "B2" (Pliocene sand and sandstone) and geoelectrical layer "C1" (Eocene limestone).*

The interpreted results of the 2-D imaging profiles and the VES curves are consistent with: (1) small thicknesses for the Pliocene aquifer in the south compared to those in the north, (2) fault control in the western part that is responsible for terminating the Pliocene aquifer against the Pliocene clay (second site).

Five normal faults were detected from the constructed cross-sections. These faults contribute to the groundwater potential in the area and act as conduits facilitating groundwater recharge at some regions and as impervious boundaries at other sites.

These effects can be illustrated by the increment of the thickness of the Quaternary aquifer in the western part comparable with the eastern part. The Quaternary aquifer in the west is recharged by the seepage from the Nile River, which has the same level as the groundwater. On the other hand, in the east the aquifer is recharged from occasional surface water flooding. Different aquifers are interconnected hydrogeologically due to the structural effect, i.e. between the Quaternary aquifer (layer A3) and the Pliocene aquifer (layer B2) in the west, and between the Pliocene aquifer (layer B2) and Eocene water-bearing (layer C1) in the east.

The uplifted clay layer (B3) at the middle of the study area subdivided the sources of recharge along the Pliocene aquifer into two different zones. A permanent recharge from the Quaternary aquifer that is feeded by the seepage from

the River Nile in the west and a seasonal one from the Eocene interconnected water-bearing limestone (low potential) that feeds through deep structures and fractures. The fault reduces the thickness of uplifted Pliocene aquifer to a small value (8.5 m at VES 3); hence, low potential for groundwater is expected at this site. Also, the Quaternary aquifer was not detected in the southern soundings due to the impact of faulting.

As the Quaternary aquifer has a greater thickness (more than 20 m) and recharged by seepage from the Nile River, a permanent source of recharge for groundwater is guaranteed. At the same time the western part of the Pliocene aquifer is feeding from the Quaternary aquifer. This in turn will store a permanent source of groundwater which is considered one of the essential requirements of sustainable development. Therefore, the western part is more suitable for the sustainable development in the area of study.

***Key words**: Aquifer, recharge, imaging profile, Vertical Electrical Sounding (VES), faults, seepage, water flood, fracture, development, interconnected water-bearing*

1- INTRODUCTION

In the last few years, the area east of El Teben that lies along Wadi Garawi has attracted many investments in different fields, especially in industries, agriculture, and mining ventures. Groundwater in this district represents the backbone of the different development projects. Evaluating the groundwater potential of the different aquifers and their sources of recharge along the Wadi will impact to some extent the future of the development plans in this area.

Wadi Garawi lies along the eastern desert side of the Nile river and debauches into the Nile river at the El Teben area (Figure1). The area of study is located between latitudes 29° 44' 30" and 29° 48' 30" N and longitudes 31° 17' 30" and 31° 25' E (Figure 1). This area is located in the arid to semi-arid belt of Egypt which is characterized by long, hot summers and short, warm winters, low rainfall and high evaporation rates. The average temperature varies from 37°C in summer (August) to about 15°C in winter (January). The annual rainfall ranges from 4.2 mm to 17.4 mm. The highest value of relative humidity is 71.8 % in December. On the other hand, evaporation generally varies from 18.7 mm/day in May to 2.3 mm/day in December (Khaled and Al Abaseiry, 2003).

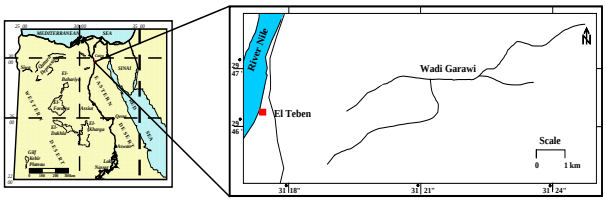

Figure (1): Location map of the study area.

1- Geomorphological Aspects:

Topographically, the study area is characterized by moderate to low relief where its surface is generally sloping from east to west, i.e. towards the Nile River (from about 100 m to 20m). The geomorphological parameters of the area east of Cairo were determined by Said and Beheiri (1961). Three geomorphic units were identified by Said (1962). These units are the young alluvial plain, the old alluvial plain, and the calcareous structural plateau. The young alluvial plain comprises the old cultivated land of the Nile valley, irrigation canals and drains. They run generally parallel to the course of the Nile. The old alluvial plain extends easterly between the young alluvial plain and the calcareous structural plateau. This plain includes good soils in elevated terraces suitable for reclamation processes. Three pediments, plateaus, scarps, ridges and low lands are the main landforms. The calcareous structural plateau constitutes the eastern boundary of the studied area and extends to the Red Sea Mountains. Its composition is of Eocene limestone deposits. It is dissected by a number of wadis directed toward the Nile River. Wadi Garawi is one of these wadis. Generally, the drainage density is low indicating more or less gentle stream erosion (Abd-El Shafy et al., 1986).

2- GEOLOGICAL SETTING

The outcrop deposits in the area of study range in age from Quaternary to Eocene (Figure 2). The description of these deposits is as follows:

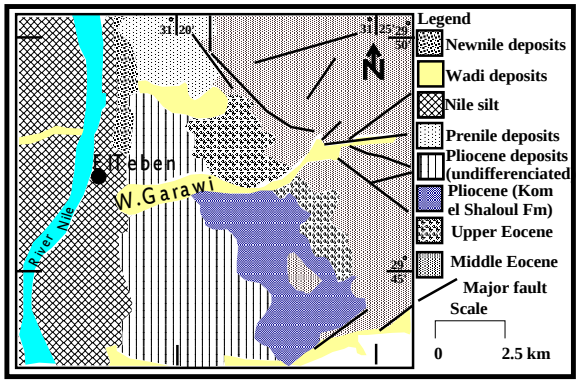

Figure (2): Geologic map of the study area and vicinity. (CONOCO, 1987)

Pleistocene deposits; these deposits form terraces of different elevations above the flood plain (ProtoNile, PreNile and NewNile sediments). These deposits conformably overly the Pliocene deposits and form the main water bearing formation east the Nile River

Plio-Pleistocene deposits; have a wide distribution on the eastern side of the Nile Valley between the El Kuraimat and El Saff areas (Said, 1981). These deposits consist mainly of conglomerates.

Pliocene deposits; consist of a thick series of interbedded clay and thin, fine-grained sand and silt lamina which crop out along the banks of the valley and many of the wadis. These sediments occur below the Pleistocene deposits and serve as a thick impermeable to semi- impermeable zone below Pleistocene water-

bearing sediments. Pliocene deposits are represented by two units according to El Sayed (1993) as follow:

- Undifferentiated sand and clay sediments
- Kom El Shelul Formation which is made up of sandstone and coquinal limestone beds. This formation overlies unconformably the Eocene Rocks.

Eocene rocks are distributed in the eastern fringes of the study area forming the high plain structures extending further to the east. These rocks are divided into two main units. The upper one is represented by the Upper Eocene (Maadi Formation) and consists of shallow marine shale and limestone with intercalations of marine sandstone. The Lower unit is represented by Middle Eocene (Mokattam group unit) which is made up of dense bedded limestone with local chert and few nummulites.

Structurally, faulting forms the main structural elements in the study area. These faults have E-W, NE-SW and NW-SE trends. They have a great impact on the groundwater conditions east of the Nile River along the study area. Minor associated folds have been recognized in the eastern portion and are oriented NW-SE (Shukri, 1953).

3- HYDROGEOLOGICAL SETTING

The hydrogeological setting of the concerned aquifers was studied by Abdel Shafy et.al.(1986), El Sayed (1993), and Youssef (2007). Three types of aquifers were reported in the study area: the Quaternary, Pliocene and Eocene aquifers.

The Quaternary aquifer consists of Pleistocene sand and gravels intercalated with clay lenses. Its thickness increases from a few meters at the eastern fringes of the Nile to several tens of meters close to the course of the Nile. The groundwater occurs under semi-confined conditions due to the presence of a semi-pervious clay layer capping the aquifer. The semi-confined condition prevails in the old cultivated lands (PreNile aquifer). The unconfined conditions prevail in the areas where the Quaternary sediments outcrop and along the trunks of the main Wadis that extend easterly to the borders of the east plateau. The Quaternary aquifer is generally recharged from the upland floods, the recent and old Nile floods, seepage of irrigation canals and from cultivated lands.

The Pliocene aquifer consists of conglomerates mixed with sand and shale intercalations (El Sayed, 1993). It ranges in thickness from 40m-120m. It is mainly recharged from the eastern highlands as well as the adjacent Quaternary aquifer. It overlies Pliocene clay. Sometimes this clay encloses sand lenses containing pockets of groundwater (Awad 1999).

The Eocene limestone aquifer was detected as water-bearing in some areas where marine shale and limestone with intercalation of marine sandstone were detected. It exists under Pliocene deposits in the Nile Valley and outcrops to the east forming a high plateau. This aquifer has low potential and the water salinity is high (2500-8000 ppm). Possible recharge from ancient floods may have occurred, as well as upward leakage from the deep aquifers and through deep fractures.

The hydrochemistry of the groundwater in the study area and its surroundings have been discussed by El Sayed. et al. (2004) and El Sheikh (2008). According to them, the Quaternary aquifers have fresh to fairly brackish groundwater (< 1000 ppm to 2500 ppm). Salinity increases eastward due to the mixing with groundwater of the Pliocene aquifer. The Pliocene aquifer has brackish salinity (3000-5000 ppm) where the Pliocene clay sediments play the main role in increasing the salinity (El Sheikh, 2008).

4- GEOELECTRICAL STUDIES

Field work and interpretation:

The field work in the area of study includes both Vertical Electrical Soundings and Two-Dimensional Electrical Imaging profiles.

A-Vertical Electrical Sounding

A total of 20 Vertical Electrical Soundings (VES) were carried out in the investigated area (Figure3). Sounding station nos. 1, 5, 16 and 20 were conducted beside drilled wells to correlate or calibrate the geoelectrical units with the major sedimentary units for the water-bearing Pliocene and Quaternary deposits. Similarly, sounding station nos. 8 and 9 were conducted beside hand dug wells to link lithology and resistivity for Quaternary alluvial water-bearing aquifers. Also, sounding station nos. 2 and 4 were located near some existing quarries to benefit from information visible in the lithological successions at these locations for interpreting and constraining the geoelectrical models. The distances between sounding stations are variable. The sounding stations were more concentrated around the quarries to take advantage of the available field relations in these areas. The Schlumberger configuration was applied with a distance between the two current electrodes starting from 2 meters and reaching up to 1400 meters. The Terrameter SAS 300 resistivity meter was used during this survey for measuring the resistance "R".

Topographic surveying was carried out to accurately locate the sounding stations and to determine their ground elevations from the topographic map with a scale of 1: 100,000.

Interpretation of the Vertical Electrical Sounding data:

The field data of the vertical electrical sounding has been interpreted qualitatively and quantitatively to delineate the subsurface sequence of the geoelectrical layers:

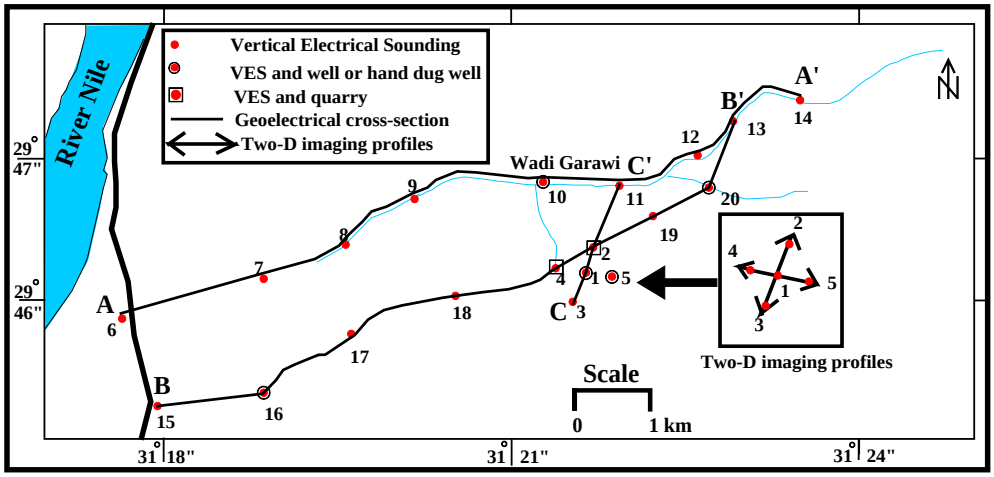

Figure (3): Location map of VES stations and geoelectrical profiles.

-Qualitative interpretation

Qualitative interpretation includes comparison of the relative changes in the apparent resistivity and thickness of the different layers. It gives information about the number of layers, their continuity homogeneity or heterogeneity of the individual layers.

The field curves of the Vertical Electrical Soundings are variable along the area of study. The areas of study are characterized by HK, KH, Q and H type curves (Figure 4), indicating surface and near surface variations or heterogeneity of the topmost layers. Also, the last segment of the VES curves shows K-type, Q-type and H-type curves. Both K-type and Q-type curves indicate a low resistivity layer. On the other hand, H-type curves reflect a high resistivity layer.

B-Quantitative interpretation

The quantitative interpretation of the geoelectrical resistivity sounding data was carried out using the computer programs "**RESIST**" (Velpen, 1988) and "**RESIX-PLUS**" (Interpex, 1996). They are interactive, graphically oriented, forward and inverse modeling programs for interpreting the resistivity curves in terms of a layered earth model. The lithologic data of the quarries near VES nos. 4 and 2 (Figs 5 and 6) as well as the hydrogeological data of the drilled wells and hand dug wells were used to help in constructing the initial models, which are needed for the geoelectrical interpretation.

Discussion of the Vertical Electrical sounding results

The quantitative interpretation of the sounding measurements that are used in constructing three cross-sections (A-A', B-B' and C-C') running in the SW-NE and S-N directions (Figures 7, 8 and 9) along the area of study led to the detection of three main geoelectrical units (A, B, and C), which correspond to Quaternary, Pliocene and Eocene deposits. The ranges of resistivities and thicknesses of each unit are listed in table 1. A description of each zone is given as follows:

Unit A

This unit corresponds to Quaternary deposits. It was differentiated into 4 geoelectrical layers (A1, A2, A3 and A4) representing different facies of Quaternary deposits. Geoelectrical layer "**A1**" consists of a group of minor layers. Its resistivity value ranges between 23 Ohm-m at VES 10 and 2265 Ohm-m at VES 13. The low resistivity value corresponds to the clayey sand deposits of the Quaternary alluvium whereas the high resistivity value corresponds to boulders, gravel, sands and sandstone. The thickness of this zone varies from 2.5 m at VES 8 to 12.6 m at VES 1.

The geoelectrical layer "**A2"** has a resistivity value that varies from 1.9 Ohm-m at VES 9 to 5.7 Ohm-m at VES 13. The low resistivity value of this layer corresponds to clay deposits. The thickness of this geoelectrical layer ranges between 2.5 m at VES 12 and 6.4 m at VES 13. This layer was not detected at all of the sounding stations.

The geoelectrical layer **A3** has a resistivity value varying from 9.6 Ohm-m at VES 6 to 79 Ohm-m at VES 13 (Fig. 6). This layer represents Quaternary water-bearing deposits. The resistivity value of this geoelectrical layer generally decreases westwards (downstream direction). The low resistivity value of this layer corresponds to Nile silt and fine sand whereas the high resistivity value (in the east) corresponds to gravel and sand of alluvial deposits. The thickness of this layer varies from 5 m at VES 8 to 21.3 m at VES 16 at the extreme west (direction of increasing thickness). This geoelectrical layer was not detected at VES nos. 1, 2, ….., 5 and 14.

The geoelectrical layer **A4** has a resistivity value ranging from 1 Ohm-m at VES 3 to 9.7 Ohm-m at VES 2. The resistivity value of this layer corresponds to clay to sandy clay deposits. The thickness of this geoelectrical layer ranges between 3.8 m at VES 1 and 9.8 m at VES 18. This layer was not detected at the sounding stations nos. 8, 13 and 20.

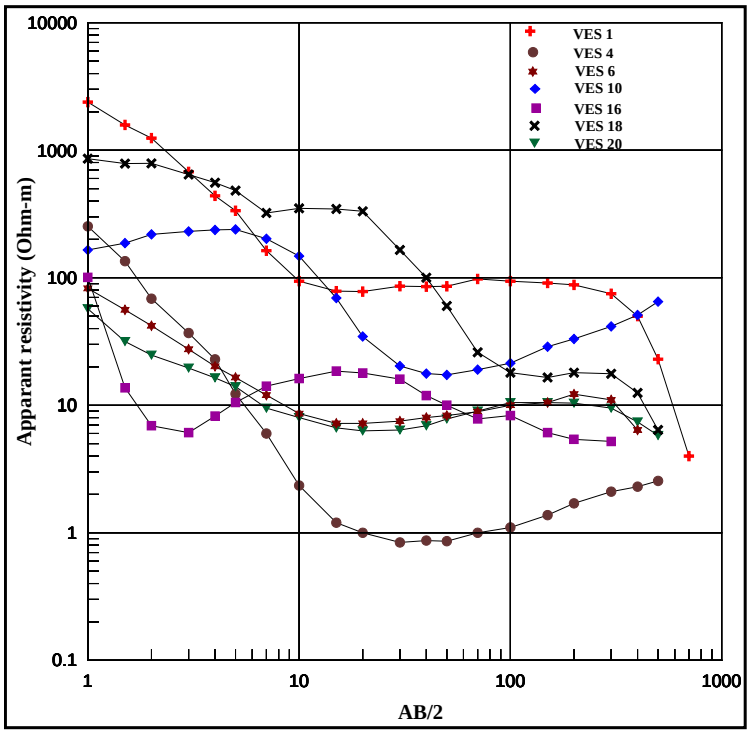

Figure (4): Field curve types in the study area.

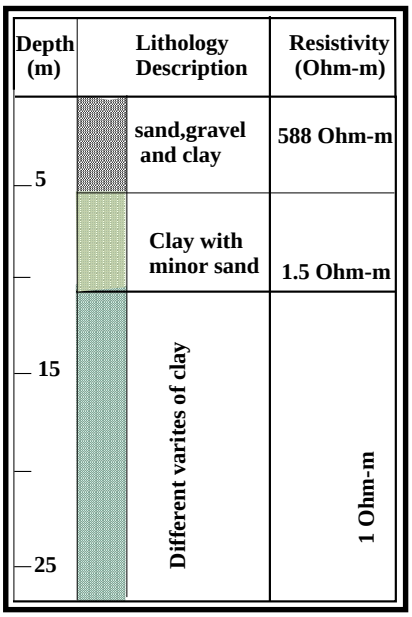

Figure (5): Lithologic cross-section. at the Quarry near VES 4.

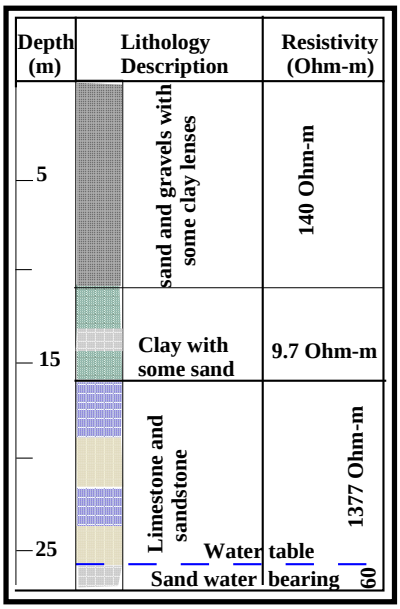

Figure (6): Lithologic cross-section. at the Quarry near VES 2.

Unit B

This unit is equivalent to Pliocene deposits. It consists of three geoelectrical layers (B1, B2, and B3) representing different facies of Pliocene deposits. Geoelectrical layer "B1" has a resistivity value that varies from 45 Ohm-m at VES 9 to 1621 Ohm-m at VES 1. This resistivity value corresponds to dry limestone and sandstone of Pliocene age, as described from the Quarry at VES no. 2. Generally, this layer has a high resistivity value. An anomalously low resistivity value (<100 Ohm-m) was detected only at VES nos. 3 and 9. This layer has a thickness varying from 5 m at VES 9 to 10.4 m at VES 3.

The geoelectrical layer B2 has a resistivity value varying from 11.2 Ohm-m at VES 9 to 60.5 Ohm-m at VES 2 (Figs. 7, 8, and 9). This layer represents Pliocene water-bearing sandstone, sand and clay as indicated from the drilled wells in the area of study and the quarry near VES no. 2 that reaches to the water table of this layer. The low resistivity value of this layer is due to the clay with sand and/or increasing salinity of groundwater. This geoelectrical layer was not detected at VES nos. 4, 13, 16 and 20. The thickness of this layer varies from 8.5 m at VES 3 to 35 m at VES 2.

The geoelectrical layer "B3" has a resistivity value ranging from less than 1 Ohm-m at VES 1 to 6.6 Ohm-m at VES 12. The resistivity value of this layer corresponds to clay deposits. This layer was detected with minor thickness at VES nos. 13, 14 and 20 (6m-7m) whereas 44 m was penetrated at VES no 4 and its base unreached with the applied current electrode separation at this sounding and at the other sounding stations.

Unit C

The last detected unit corresponds to Eocene rocks. This unit consists of two geoelectrical layers and was detected only at the extreme east at VES nos. 13, 14 and 20. The first geoelectrical layer "C1" has a resistivity value varying from 34.5 Ohm-m at VES 20 to 65 Ohm-m at VES 13. This layer corresponds to fractured water-bearing Eocene limestone. The relatively low resistivity value is due to shale mixed with the limestone. This layer has a uniform thickness (45 m at VES 20 to 47 m at VES 14). The second geoelectrical layer "C2" has a resistivity value that varies from 116 Ohm-m at VES 20 to 199 Ohm-m at VES 14. This layer corresponds to massive Eocene limestone. The base of this layer was undetected with the current electrode separation used.

To avoid repetition, the main findings reached from the constructed geoelectrical cross sections are given in the following:

- The geoelectrical layer "A4" was not detected at VES nos. 8, 13 and 14. Similarly geoelectrical layers "B1 and B2" were not detected at VES nos. 13 and 14 due to the effect of faults.
- The thickness of Quaternary water-bearing layer "A3" is small along the main channel. Its thickness increases at the western part (VES nos. 6, 7, 15 and 16) and the deposits decrease in resistivity relative to the main channel. This is due to their lithological composition being finer than the main channel deposits.
- The Quaternary water-bearing layer "A3" was not detected at the southern soundings (cross section B-B') except at VES nos. 13 and 20 at the extreme east. and VES nos. 15 and 16 at the extreme west due to faulting effects.
- The section at VES no. 4 consists mainly of clay that lies below the surface wadi fill deposits layer "A1". This clay laterally contacts limestone, sandstone and sand of Pliocene age on the sides of the wadi.
- Unit "C", Eocene limestone, was detected only at the extreme east (VES nos. 13, 14 and 20).

B- Two-Dimensional Electrical Imaging

Two profiles were carried out because the quarries near VES nos. 2, 4 and 5 showed variation in exposed lithologies. One of the main objectives of this study was to detect the horizontal and vertical variations in the subsurface lithology and to understand the distribution and impact of structural elements in the study area on the groundwater occurrence and recharge. The geoelectrical imaging method has been widely used in environmental and geotechnical investigations for mapping complex geological structures (Griffiths and Barker, 1993). The number of multiple electrode spacing used depends on the length of the traverse and the maximum depth of investigation (Edwards, 1977). The Wenner array of electrodes system was adopted in the investigation. Each profile has a length of 900 m. The unit electrode separation was 15 m which was increased at each traverse by one unit to reach a maximum spacing of 300 m (i.e. 15, 30, 45, ..., 300 m). The first profile trends more or less in a NE-SW direction and passes by VES nos. 3, 1 and 2 respectively. The second profile trends approximately W-E and passes through VES nos. 4, 1 and 5. The 2D resistivity survey was performed at the proposed sites using a Terrameter SAS 1000 resistivity meter and a multicore cable to which electrodes were connected at takeouts molded on at predetermined equal intervals. A computer-controlled system was then used to select the active electrodes for each electrode set-up automatically (Griffiths, Turnbull and Olayinka, 1990).

Interpretation Results of the Two-Dimensional Imaging Data

The computer program RES2DINV, ver. 3.4 written by Loke (1998) has been used for the interpretation of the 2-D resistivity data. It is a Windows-based computer program that automatically determines a two-dimensional (2-D) subsurface resistivity model for data obtained from electrical imaging surveys (Griffiths and Barker 1993).

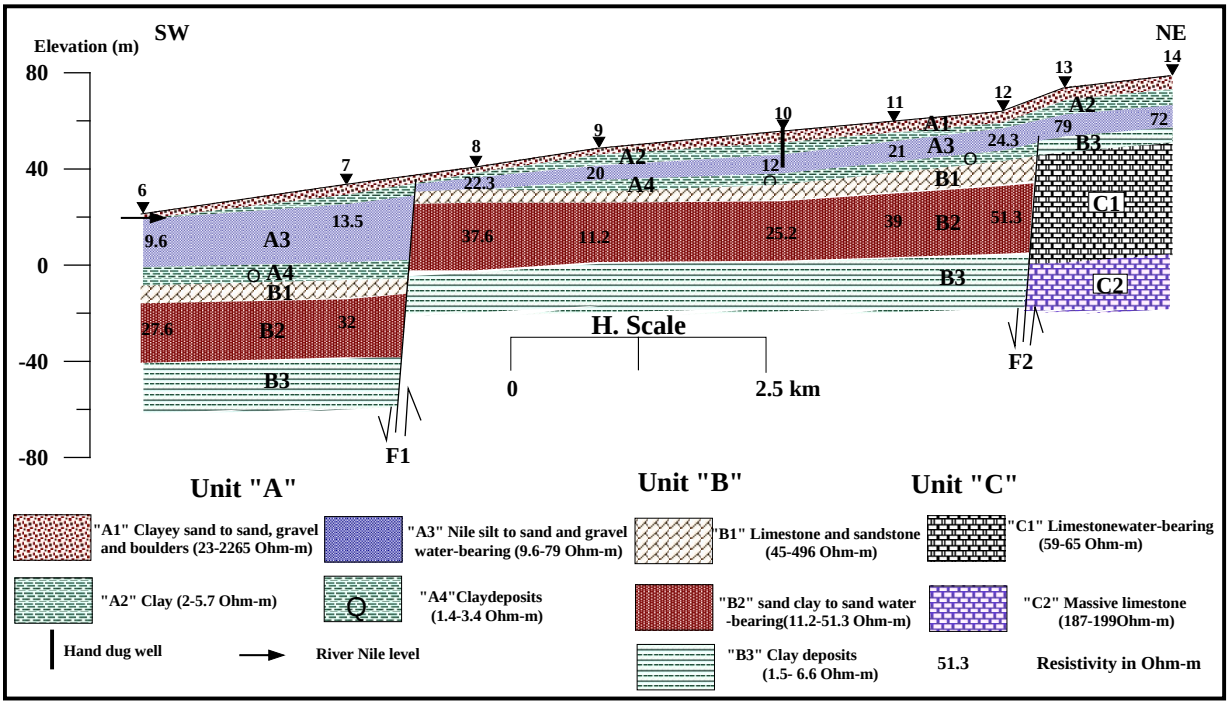

Figure (7): Geoelectrical cross-section A-A'.

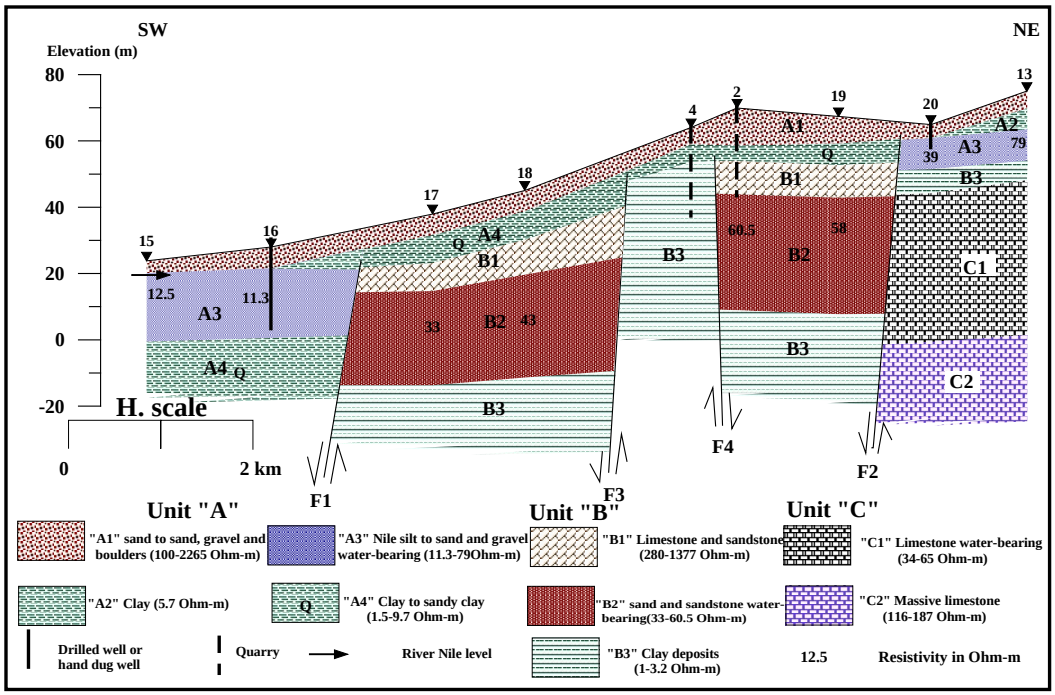

Figure (8): Geoelectrical cross-section B-B'.

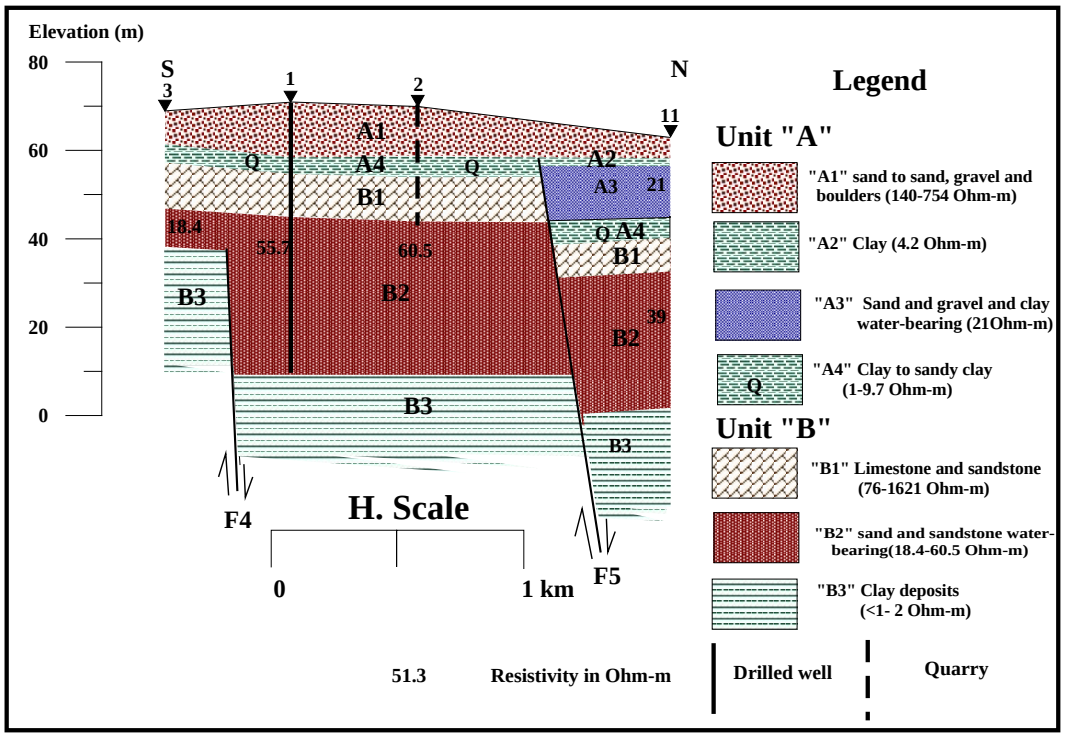

Figure (9): Geoelectrical cross-section C-C'.

Table (1): Resistivity and thickness ranges.

Unit	Layer	Resistivity (Ohm-m)	Thickness (m)
"A"	A1	13 (VES 10) 2265 (VES 13)	2.5 (VES 8) 12.6 (VES 1)
	A2	1.9 (VES 9) 5.7 (VES13)	2.5 (VES 12) 6.4 (VES 13)
	A3	9.6 (VES 6) 79 (VES 13)	5 (VES 8) 21.3 (VES 16
	A4	1 (VES 3) 9.7 (VES2	3.8 (VES 1) 9.8 (VES 18)
"B"	B1	45(VES9) 1621(VES 1)	5 (VES 9) 10.4 (VES 3)
	B2	11.2 (VES 10) 60.5 (VES 2)	8.5 (VES 3) 35 (VES 2)
	B3	<1 (VES 1) 6.6 (VES 12)	6 (VES 13) >44 (VES 4)
"C"	C1	34.5 (VES 20) 65 (VES 13)	45 (VES 20) 47 (VES 14)
	C2	116 (VES 20) 199 (VES 14)	

A forward modeling subroutine is used to calculate the apparent resistivity values and a non-linear least-square optimization technique is used for inversion routine (De Groot-Hedlin and Constable, 1990 and Loke and Barker 1996a)**.**

The interpretation results of the inverse model resistivity section at the first site passing through VES nos. 3, 1 and 2 (Fig. 10) revealed lateral and vertical variations in resistivity values. The near-surface lithology has high resistivity and corresponds to Quaternary wadi-fill deposits, sandstone and limestone of Pliocene age. The details of near-surface variations were undetected with the electrode separations used. The underlying zone represents the water-bearing formation of Pliocene age. This zone extends to depths varying from about 25 m at the extreme south to about 70 m in the area between VES nos. 1 and 2. This zone shows variation in resistivity from 13 ohm-m to about 100 Ohm-m. An anomalously high resistivity value (> 120 Ohm-m) beneath electrode locations 510 - 720m was detected. This high resistivity value may be related to the presence of highly cemented sandstone patches. The thickness of this zone decreases southward perhaps due to the presence of a fault between VES nos. 1 and 3. The third zone rests below the Pliocene water-bearing unit, and has low resistivity which is interpreted as clays of Pliocene age. This clay has resistivity values ranging from less than 1 Ohm-m to about 7 Ohm-m. The depth to this zone decreases southward.

The interpretation results of the inverse model resistivity section at the second site passing through VES nos. 4, 1, 5 (Fig. 11) revealed rapid lateral and vertical variations in resistivity. The near-surface lithology has high resistivity values (>125 Ohm-m) beneath electrode locations 270-900 m and is interpreted as corresponding to Quaternary wadi fill deposits, sandstone and limestone of Pliocene age. Low resistivity values (3-25 Ohm-m) were detected beneath electrode locations of 1-270 m, and are here interpreted as being dominated by clay lithologies. This layer is followed by a water-bearing zone of Pliocene age at depths ranging from about 40 m at the electrode location 335 m at the west to about 70 m in areas east of VES nos. 1 (beneath electrode location of 510 m). This zone shows variations in resistivity ranging from 10 ohm-m to more than 80 Ohm-m. Anomalously high resistivity values (> 125 Ohm-m) were detected beneath electrode locations 510- 615m that could be related to the presence of a sandstone layer of low porosity. The thickness of this zone decreases westward and is undetected in the western part where low resistivity Pliocene clay deposits (<1 Ohm-m – 6 Ohm-m) were detected, perhaps due to the presence of fault-related vertical displacement between VES nos. 4 and 1.

Groundwater occurrence:

As mentioned before, the water-bearing formations in the area of study are represented by Quaternary wadi fill deposits (geoelectrical layer A3), Pliocene sand and sandstone (geoelectrical layer B2) and Eocene limestone (geoelectrical layer C1).

The Quaternary aquifer is found in the main channel and the lower reaches of Wadi Garawi (western part). It is composed of gravels; sand, and clay in the main channel and Nile silt and fine sand at the western part. The results of the interpreted geoelectrical data indicate that the depth to the top of Quaternary water-bearing layer "A3" ranges from 4.2 m at VES 20 to 13 m at VES 14 and the water level (elevation) varies from 37 m at VES 8 at the west to 67 m above sea level at VES 14 at the extreme east along the main channel soundings. Therefore the groundwater flows regionally from the east to the west. On the other hand, in the western part that borders the Nile River, the depth to the Quaternary aquifer ranges from 3 m at VES 6 to 6.5 m at VES 16 and the water level is 20 to 20.5 m above sea level, or equivalent to the level of the Nile River. Therefore, the seepage from the Nile River recharges the Quaternary aquifer along its western border. This layer is located under an unconfined condition. The resistivity values of geoelectrical layer A3 range between 12 Ohm-m at VES 10 and 79 Ohm-m at VES13 with a general decrease in resistivity westwards along the main channel. In the western part the resistivity ranges between 9.6 and 11.3 Ohm-m, corresponding to Nile silt and fine sand.

The thickness of the Quaternary water-bearing layer is generally thin, varying from 5 m at VES 8 to 9.5 m at VES 20 along the main channel, whereas in the district bordering the Nile River a greater thickness was recorded (20.3m - 21.3 m). This aquifer was not detected in the soundings south the main channel (VES nos. 1, 2, 3, 4, 5, 17, 18 and 19), apparently due to the effects of faulting. This aquifer is present under semi-confined condition along the main channel but under confined to unconfined conditions in the western part. This water-bearing layer in the main channel is unconnected with the western part that borders the Nile River due to the effects of a fault.

Second water–bearing layer (geoelectrical layer B2)

The depth to the top of this layer ranges from 15.9 m at VES 8 to 39.5 m at VES 6 at the extreme east. The water level (msl) in this layer varies from 16.5 m at VES 6 to 46.6 m at VES 3. This layer presents semi-confined conditions where it underlies low to massive limestone and sandstone. The resistivity values of geoelectrical layer B2 ranges between 11.2 Ohm-m at VES 9 and 60.5 Ohm-m at VES 2. It is obvious that the higher resistivity value indicates sand and sandstone composition and therefore relatively better water quality. On the other hand, the low resistivity values indicate either an increase in the clay content in the sand and/or an increase in salinity; hence lower water quality is expected. The thickness of this water-bearing layer is variable. It varies from 8.5 m at VES 3 to 35 m at VES 2 due to the effect of faults. This water-bearing layer was undetected at VES nos. 13, 14 and 20 at the extreme east, and at VES 4 at the middle part due to the impact of faulting. Also the top of this layer was not reached at VES nos. 15 and 16 with the maximum current electrode separation used.

Third water–bearing layer (geoelectrical layer C1)

The third water-bearing layer is represented by Eocene limestone. This layer was detected at the extreme east of the study area (VES nos. 13, 14 and 20). This layer was detected below Pliocene clay at depths varying from 21 m at VES 20 to 27 m at VES 13. The resistivity of this water-bearing layer ranges from 34.5 Ohm-m to 65 Ohm-m. The low resistivity is related to lenses of shale within the limestone and/or increasing salinity. This layer has a uniform thickness of 45-47 m. This aquifer has low potential and the water salinity is high as discussed before.

Structural impact on the groundwater occurrence and source of recharge

In order to provide a good insight into the structural configuration in the investigated area, the results of the constructed geoelectrical cross sections have been used to generate a structural map of the study area (Figure. 12). It is relevant that the detected faults from the constructed geoelectrical cross sections (F1, F2, ….. F5) have different trends. The faults F1, F2 and F3 have NE-SW trends with their downthrown sides to the west. The fault F4 has a NW-SE trend with its eastward side downthrown. The last fault, F5, has more or less E-W trend, with its north side downthrown. These trends play an important role on the groundwater occurrence and sources of aquifer recharge in the study area. The fault "F1" uplifted the sedimentary succession in its eastern side. Therefore, the Quaternary aquifer is found with small thickness (5 - 9.5 m) east of the fault compared with a larger thickness west the fault (>20m). The Quaternary aquifer east of the fault F1 is juxtaposed against the Quaternary clay on the other side. The Quaternary aquifer east of fault F1 (along the main channel), recharges from the flooded surface water and the local precipitation. By contrast, the Quaternary aquifer (layer A3) west of fault F1 recharges by seepage from the Nile River where the water level west of fault F1 is the same as that of the Nile River (cross sections A-A' and B-B', Figs. 7 and 8).

The Pliocene aquifer (layer B2) east of fault F1 meets the Quaternary aquifer (layer A3) on the other side of the fault. Therefore, the two aquifers are hydrologically interconnected. The fault "F2" uplifted the Eocene limestone water bearing layer (C1) at the extreme eastern part in the area against the Pliocene aquifer (layer B2). Therefore, the two water-bearing layers (B٢ and C1) are hydrologically interconnected at that location. Thus the Pliocene aquifer does not exist east the fault F2 in the extreme east.

The Eocene limestone water-bearing layer is probably recharged from ancient floods and upward leakage from the deep aquifers and through deep structures and fractures. The Pliocene aquifer (B2) is expected to recharge from Eocene water-bearing layer (C1) at the extreme eastern part. Therefore, the vertical fractures have a central role in recharging limestone rocks and the lack of continuous vertical flow paths causes aquitards to act as effective confining units (Eaton and Bradbury, 2003). Vertical fracture frequency depends on layer thicknesses (Pollard and Aydin, 1988; Narr and Suppe, 1991; Gross et al. 1995, and Renshaw, 1997).

The faults "F3" and "F4" (cross section B-B' in Fig. 8) lead to the formation of domal structure at VES 4. This in turn causes the uplifted Pliocene clay layer (layer B3) between the two faults (at VES 4) to meet the Pliocene aquifer at the other sides of the two faults. Therefore the clay layer (at VES 4) divided the recharge along the Pliocene aquifer in cross section B-B' (Fig. 8) into two sources. East of this clay the source of recharge is essentially from the Eocene water-bearing layer (layer C1) that meets the Pliocene aquifer west of fault F3, and upward leakage from the deep aquifers through deep structures and fractures. On the other hand, the source of recharge west of this clay is from the Quaternary aquifer (layer A3) that meet the Pliocene aquifer (layer B2) east of fault F1 and from upward leakage from deep aquifers. The same concept of recharge through the Pliocene aquifer (layer B2) is present in cross section A-A' (Fig. 7) at VES 10 (north of VES 4) where the sandy clay composition (low resistivity of 11.2 Ohm-m) partially prevents further extension of the recharge source from the Quaternary aquifer east of this sounding (VES 10). Therefore, the clay at VES nos. 4 and 10 divided the source of recharge along the Pliocene aquifers into two different sources. The area west of these two sounding have a permanent source of recharge from the Nile River (Fig. 13) through the Quaternary aquifer. On the other hand the area east of the two soundings has a seasonal source of recharge from the Eocene water-bearing layer (layer C1) and upward leakage from the deep aquifers through deep structures and fractures.

The fault "F4" between VES nos. 1 and 3 reduces the thickness of the uplifted Pliocene aquifer (layer B2) at VES 3 to a minimum (8.5 m). This fault "F4" positions the Pliocene aquifer east of fault "F4" against a thin part of the Pliocene aquifer and Pliocene clay west of the fault. Therefore the Pliocene aquifer at VES 3 has poor potential for groundwater.

The fault "F5" between VES nos. 1 and 11 uplifted the sedimentary succession south the fault. This in turn caused the Quaternary aquifer (layer A3) on the north side of the fault (downthrown side) to meet massive limestone and sandstone on the southern part (upthrown side). Due to the action of this fault the Quaternary aquifer was not detected in the southern cross section B-B' (Fig. 8).

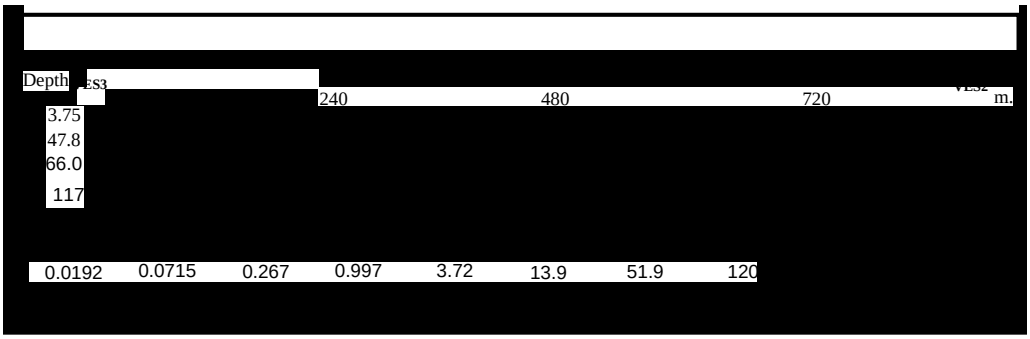

Figure (10): Interpreted Two-Dimensional imaging section at the first site.

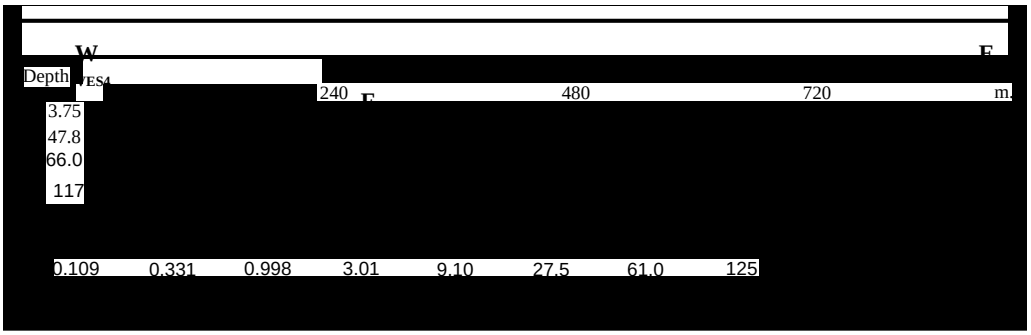

Figure (11): Interpreted Two-Dimensional imaging section at the second site.

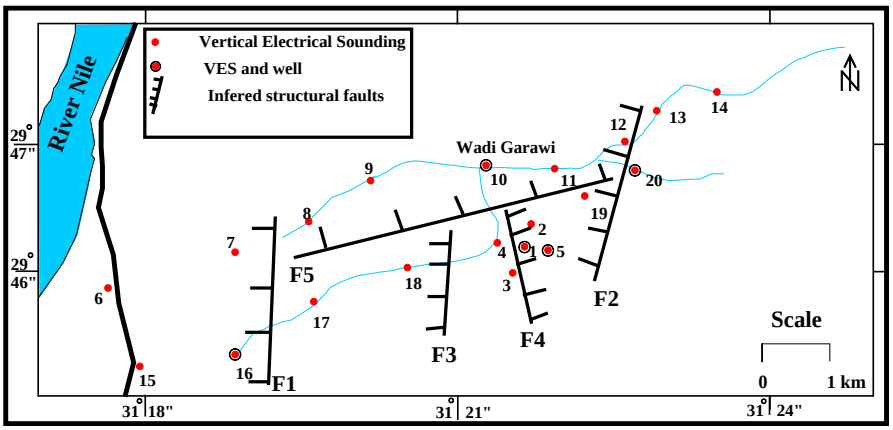

Figure (12): Structure map along the Wadi Garawi area.

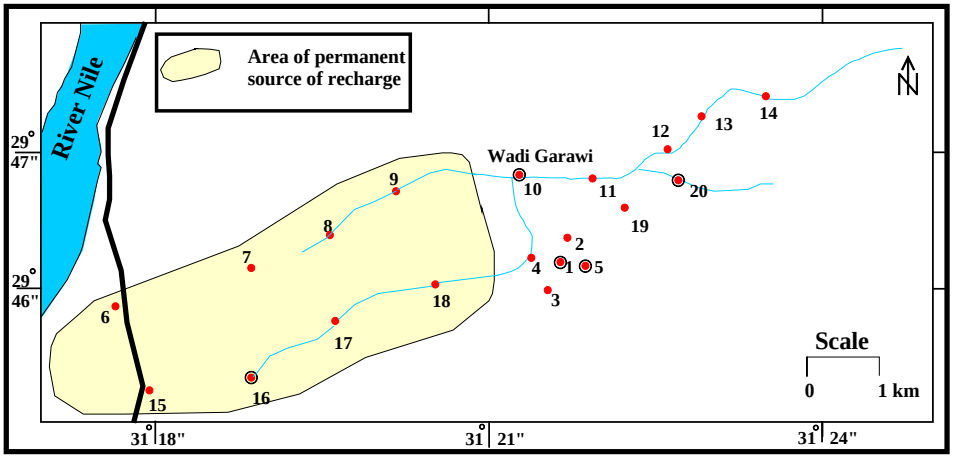

Figure (13): Inferred area of permanent source of recharge.

5- SUMMARY AND CONCLUSION

Wadi Garawi is located east of El Teben and drains into the Nile River. This area has low to moderate relief with a general westward slope. Three geomorphic units, including the young alluvial plain, the old alluvial plain and the calcareous structural plateau characterize the study area. The stratigraphic succession along the area of study comprises rock units varying in age from Quaternary to Eocene. Faults represent the main structural element in the study area. These faults have E-W, NE-SW and NW-SE trends. Three types of aquifers are described in the study area and its vicinity. These are the Quaternary, Pliocene, and Eocene aquifers.

To detect the structural impact on the potential of groundwater, and the sources of aquifer recharge, geoelectrical surveys in the form of Vertical Electrical Soundings (20 VES's) as well as 2-D imaging profiles (two cross-sections) were conducted over the study area. The quantitative interpretation of the geoelectrical resistivity sounding data as well as the constructed three geoelectrical cross sections led to the detection of three main geoelectrical units (A, B and C), which correspond to Quaternary, Pliocene, and Eocene deposits. According to this study, the geoelectrical layer A3 (part of the Quaternary alluvium deposits), geoelectrical layer "B2" (Pliocene sand and sandstone) and geoelectrical layer "C1" (Eocene limestone) represent the water-bearing formations in the area of study.

The interpreted results of the 2-D imaging profiles revealed that the thickness of the Pliocene aquifer decreases southward at the first site and the Pliocene aquifer in the eastern part is apparently faulted against the Pliocene clay in the western part at the second site. These profile results are compatible with the interpretations of the discrete VES stations.

Five normal faults were detected or inferred from the three constructed geoelectrical cross sections (F1, F2, . ….. F5). They have different trends; F1, F2 and F3 having NE-SW trends. On the other hand, F4 has a NW-SE trend. Finally, F5 trends approximately E-W. These trends play an important role on the groundwater occurrence and sources of aquifer recharge in the study area. This can be summarized as follows:

- The fault F1 has its west side downthrown. This fault increases the thickness of the Quaternary aquifer (to more than 20 m) west of the fault plane, compared with a smaller thickness (5 - 9.5 m) east of the fault. The Quaternary aquifer east of fault "F1" recharges from the flooded surface water and the local precipitation. By contrast, the Quaternary aquifer (layer A3) west of fault F1 recharges from the seepage of the Nile River where the water level west of fault F1 is the same as that of the Nile River. The Pliocene aquifer (layer B2) east of fault F1 is placed against the Quaternary aquifer (layer A3) on the other side of the fault. Therefore, the two aquifers are interconnected.

-The fault "F2" has its west side downthrown. It uplifted the Eocene limestone water-bearing layer (C1) at the extreme eastern part in the area of study area against the Pliocene aquifer (layer B2). Therefore, the two water-bearing layers (B3 and C1) are hydrologically interconnected. The Eocene limestone water-bearing layer was probably recharged from ancient floods and upward leakage from the deep aquifers via deep structures and fractures.

Faults F3 and F4 with downthrown sides to the east and west, respectively, uplifted the Pliocene clay layer (layer B3) between the two faults (at VES 4) to meet the Pliocene aquifer at the other two sides. Therefore, the uplifted clay layer (at VES 4) divides the recharge sources along the Pliocene aquifer in cross section B-B' into two regions. East of this clay the source of recharge is essentially from the Eocene water-bearing layer (layer C1) and upward leakage from deep aquifers through fractures and faults. On the other hand, the source of recharge west of this uplifted clay is from the Quaternary aquifer (layer A3). The same concept of recharge through the Pliocene aquifer (layer B2) can be inferred from cross section A-A' at VES 10 (north of VES 4) where the sandy clay composition (low resistivity of 11 Ohm-m) at this location is expected to reduce the area of the recharge source from the Quaternary aquifer east of this sounding (VES 10). Therefore the uplifted clay at VES nos. 4 and 10 split the source of recharge of the Pliocene aquifers into two different regimes; a permanent source of recharge from the Nile River through the Quaternary aquifer, and a seasonal source of recharge from the Eocene water-bearing layer (layer C1).

The fault F4 between VES nos. 1 and 3 reduces the thickness of the uplifted Pliocene aquifer (layer B2) at VES 3 to a small value (8.5 m). Therefore, the Pliocene aquifer at VES 3 has poor potential for groundwater.

The fault F5 between VES 1 and 11 is down to the north. It uplifted the sedimentary succession south the fault. This in turn caused the Quaternary aquifer (layer A3) north of the fault (downthrown side) to contact massive limestone and sandstone of the southern part (upthrown side). Therefore, the Quaternary aquifer was not detected in the sounding stations south of the main channel of the wadi.

Results of this study suggest that the eastern part of the study area has low ground water potential given the small thickness (5-9.5 m) of water-bearing formation and depends on a seasonal source of recharge (seasonal floods and rain fall). The Eocene limestone aquifer that supplies the Pliocene aquifer has low potential for groundwater. On the other hand, the western part of the study area has moderate to fair potential for groundwater. As the Quaternary aquifer has a larger thickness (more than 20 m) and is recharged directly from the Nile River that guarantees a permanent source of recharge for groundwater. At the same time

the Pliocene aquifer in the western part is being recharged through the Quaternary aquifer. This in turn ensures a permanent source of groundwater which is considered one of the essential requirements of sustainable development. Therefore, the western part is more suitable for the different objectives of development in the area of study.

Well logging should be conducted in any drilled well to enable the best well design.

To achieve a safe yield for the production wells and to avoid the problem of interfering cones of depression, the distance between wells must be precisely determined (not less than 500 m) and pumping test for each well must be carried out.

REFERENCES

Abdel Fattah, T. A., 2007. Application of well log tools and organic geochemistry in source rock identification, southern Gulf of Suez, Egypt (abs.). GSA Denver Annual Meeting (28–31 October 2007).

Alsharhan, A.S., 2003. Petroleum geology and potential hydrocarbon plays in the Gulf of Suez rift basin, Egypt. AAPG Bull., 87 (1), 143–180.

Bosworth, W., Crerello, P., Winn Jr, R.D., and Steinmetz, J., 1998. Structure, sedimentation, and basin dynamics during rifting of the Gulf of Suez. In (Eds.), Purser, B.H. and Bosence, D.W.J. Sedimentation and Tectonics of Rift Basins: Red Sea – Gulf of Aden, 78-96.

Egyptian General Petroleum Corporation, EGPC, 1996. Gulf of Suez oil fields (A comprehensive overview), 736 p.

El-Shahat, W., Villinski, J. C., and El-Bakry, G., 2009. Hydrocarbon potentiality, burial history and thermal evolution for some source rocks in October oilfield, northern Gulf of Suez, Egypt. Journal of Petroleum Science and Engineering, 68, 245–267.

El Sharawy, M.S., 2006. Seismic and well log data as an aid for evaluating oil and gas reservoirs in the southern part of the Gulf of Suez, Egypt. PhD dissertation, Mansoura University, Egypt, 265 p.

Espitalie, J., Madec, M., Tissot, J., Menning, J., Leplat, P., 1977. Source rock characterization method for petroleum exploration. Proc., 9th Annual Offshore Technology Conf., 3, 439–448.

Hunt, J.M., 1995. Petroleum Geochemistry and Geology. W.H. Freeman and Company, New York. 743 pp.

Hood, A., Gutjahr, C.C.M., and Heacock, R.L., 1975. Organic metamorphism and the generation of petroleum. AAPG Bull., 59 (6), 986-996.

Khalil, B. A., 1993. Reservoir evaluation in the southern part of the Gulf of Suez and its structural relationship. Ph.D. dissertation, Ain Shams University, 247 p.

Lopatin, N.V., 1971. Temperature and geologic time as factors in qualification (in Russian): Akad. Nauk. SSSR Izv. Ser Gel., 3, 95-106.

Mallick, R.K., and Raju, S.V., 1995. Thermal maturity evaluation by sonic log and seismic velocity analysis in parts of Upper Assam Basin, India. Org. Geochem., 23 (10), 871-879.

Meyer, B.L., and Nederlof, M.H., 1984. Identification of source rocks on wireline logs by density/resistivity and sonic transit time/ resistivity cross plots. AAPG Bull. 68, 121-129.

Myers, K.J., and Jenkyns, K.F., 1992. Determining total organic carbon content from well logs: an intercomparison of GST data and a new density log method. Geological applications of wireline logs II. In (Eds), Hurst, A., Griffiths, C.M., Worthington, P.F., Geol. Soc. London, Spec. Publ., 65, 369-376.

Passey, O.R., Moretti, F.U., and Stroud, J.D., 1990. A practical model for organic richness from porosity and resistivity logs. AAPG Bull. 74, 1777–1794.

Peters, K.E., 1986. Guidelines for evaluating petroleum source rock using programmed pyrolysis. AAPG Bull. 70, 318– 329.

Robertson Research International (RRI), 1986. The Gulf of Suez area, Egypt: stratigraphy, petroleum geochemistry, petroleum geology, six volumes Robertson Group, Leandudno.

Robertson Research International (RRI), 1984. Results of "rock-eval" pyrolysis analyses of cuttings and core samples from haltenbanken well: 6507/12-1, Report no. 5406P/D, 24 p.

Robertson Research (US) Inc., 1983. Geochemical analysis of north Aleutian Shelf, Cost no. 1 well, Alaska, Report no. 823/135, 318 p.

Said, R., 1990. Cretaceous paleogeographic maps. in R. Said: Geology of Egypt, 1990, 439-449.

Salah, M.G., and Alsharhan, A.S., 1998. The Precambrian basement: A major reservoir in the rifted basin, Gulf of Suez. Journal of Petroleum Science and Engineering 19, 201–222.

Schmoker, J.W., 1981. Determination of organic-matter content of Appalachian Devonian shales from gamma-ray logs. AAPG Bull. 65, 2165–2174.

Schmoker, J.W., 1979. Determination of organic content of Appalachian Devonian shales from formation - density logs. AAPG Bull. 63, 1504-1509.

Schmoker, J.W., and Hester, T.C., 1983. Organic carbon in Bakken Formation, United States portion of Williston Basin. AAPG Bull. 67, 2165–2174.

Staplin, F.L., 1969. Sedimentary organic matter, organic metamorphism, and oil and gas occurrence. Canadian Petroleum Geology Bull., 17, 47-66.

Tissot, B.P, Pelet, R., and Ungerer, P., 1987. Thermal history of sedimentary basins, maturation indices, and kinetics of oil and gas generation. AAPG Bull., 71 (12), 1445-1466.

Tissot, B.P., and Welte, D.H., 1984. Petroleum Formation and Occurrence. Springer-Verlag, New York, 966 p.

Waples, D.W., 1980. Time and temperature in petroleum formation: application of Lopatin's method to petroleum exploration. AAPG Bull., 64 (6) (June), 916-926.